

ACCURACY OF FINITE-DIFFERENCE MODELING OF THE ACOUSTIC WAVE EQUATION

R. M. ALFORD,* K. R. KELLY,* AND D. M. BOORE ‡

Recent interest in finite-difference modeling of the wave equation has raised questions regarding the degree of match between finite-difference solutions and solutions obtained by the more classical analytical approaches. This problem is studied by means of a comparison of seismograms computed for receivers located in the vicinity of a 90-degree wedge embedded in an infinite two-dimensional acoustic medium. The calculations were carried out both by the finite-difference method and by a more conventional eigenfunction expansion technique. The results indicate the solutions are in good agreement provided that the grid interval for the finite-difference method is sufficiently small. If the grid is too coarse, the signals computed by the finite-difference method become strongly dispersed, and agreement between the

two methods rapidly deteriorates. This effect, known as "grid dispersion," must be taken into account in order to avoid erroneous interpretation of seismograms obtained by finite-difference techniques.

Both second-order accuracy and fourth-order accuracy finite-difference algorithms are considered. For the second-order scheme, a good rule of thumb is that the ratio of the upper half-power wavelength of the source to the grid interval should be of the order of ten or more. For the fourth-order scheme, it is found that the grid can be twice as coarse (five or more grid points per upper half-power wavelength) and good results are still obtained. Analytical predictions of the effect of grid dispersion are presented; these seem to be in agreement with the experimental results.

INTRODUCTION

Solutions to wave propagation problems by finite-difference methods have received considerable attention in recent years (Alterman and Karal, 1968; Ottaviani, 1971; Boore, 1970). These methods are particularly attractive for structurally complex subsurface geometries because of the great difficulties encountered in obtaining analytical solutions. Geometries of particular interest in petroleum exploration are those containing sharp corners which generate diffractions. The purpose of this paper is to examine the accuracy of finite-difference methods for treatment of geometries containing sharp corners. This is accomplished by comparing the solution of the acoustic wave equation obtained by finite-differ-

ence methods to that obtained by classical analytical methods for the simple case of an infinite two-dimensional 90-degree wedge (quarter space) in an otherwise infinite homogeneous medium. The source field was that due to a line source distribution located parallel to the corner of the wedge (see Figure 1). For analytical simplicity, the acoustic velocity of the wedge medium is taken to be zero. This is equivalent to having a perfectly "soft" wedge medium such as a vacuum.

ANALYTICAL SOLUTION

The governing equation describing the acoustic velocity potential $u(\rho, \phi, t)$ in a homogeneous region due to a line source distribution located at (ρ_s, ϕ_s) with respect to the origin of a cylindrical

Paper presented at the 43rd Annual International SEG Meeting, October 10, 1973, Mexico City. Manuscript received by the Editor January 31, 1974.

* Amoco Production Co., Tulsa, Okla. 74102.

‡ Stanford University, Stanford, Calif. 94305.

© 1974 Society of Exploration Geophysicists. All rights reserved.

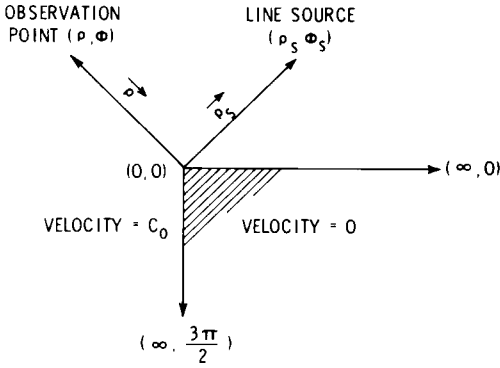


FIG. 1. Cross-section illustrating geometry and cylindrical coordinates for the 90 degree wedge model.

coordinate system is

$$\left[\nabla^2 - \frac{1}{C_0^2} \frac{\partial^2}{\partial t^2} \right] u(\rho, \phi, t) = -4\pi \frac{\delta(\rho - \rho_s) \delta(\phi - \phi_s) f(t)}{\rho} \tag{1}$$

where C_0 is the velocity of acoustic propagation in the medium, ∇^2 is the Laplacian operator, $f(t)$ is the time variation of the source distribution, and $-4\pi \delta(\rho - \rho_s) \delta(\phi - \phi_s) / \rho$ is the normalized two-dimensional Dirac delta function at the source location (Morse and Feshbach, 1953, p. 893). The Fourier transform with respect to time of equation (1) yields the reduced wave equation:

$$[\nabla^2 + k^2] U(\rho, \phi, \omega) = -4\pi \frac{\delta(\rho - \rho_s) \delta(\phi - \phi_s)}{\rho} F(\omega), \tag{2}$$

where

$$U(\rho, \phi, \omega) \equiv \int_{-\infty}^{+\infty} u(\rho, \phi, t) e^{-i\omega t} dt,$$

$$F(\omega) \equiv \int_{-\infty}^{+\infty} f(t) e^{-i\omega t} dt,$$

and

$$k = \omega / C_0.$$

The solution to equation (2) in the presence of the 90-degree wedge subject to the boundary condition of the vanishing of the acoustic velocity potential at the surface of the wedge, the requirement of boundedness at the origin, and the re-

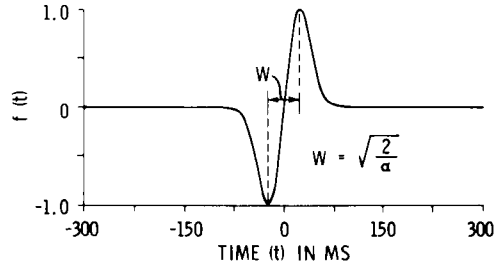


FIG. 2. Normalized source distribution time function.

quirement of outward traveling waves at infinity may be obtained by classical eigenfunction expansion techniques (Oberhettinger, 1954). The solution is available (Bowman et al, 1969, p. 265) and is given by

$$U(\rho, \phi, \omega) = \frac{-i8\pi}{3} F(\omega) \sum_{n=1}^{\infty} J_{\lambda_n}(k\rho) H_{\lambda_n}^{(2)}(k\rho_s) \cdot \sin \lambda_n \phi_s \sin \lambda_n \phi, \quad \rho \leq \rho_s, \tag{3}$$

where $\lambda_n = \frac{2}{3}n$, $H_{\lambda_n}^{(2)}$ is the second Hankel function of order λ_n , and J_{λ_n} is the Bessel function of the first kind of order λ_n . The solution for $\rho > \rho_s$ is obtained by interchanging the roles of ρ and ρ_s in the right-hand side of (3). The corresponding time domain solution to the problem is given by the inverse Fourier transform of (3); i.e.,

$$u(\rho, \phi, t) = \frac{1}{2\pi} \int_{-\infty}^{+\infty} U(\rho, \phi, \omega) e^{+i\omega t} d\omega. \tag{4}$$

The time variation of the source distribution, taken as the first derivative of a Gaussian function, is

$$f(t) = te^{-\alpha t^2}, \tag{5}$$

where α is a constant governing w the time interval from negative to positive peaks of the function as shown in Figure 2. This choice was made as a good compromise between short time duration and a narrow spectrum. The Fourier transform of (5) is

$$F(\omega) = \frac{-i\omega}{\alpha} \left(\frac{\pi}{4\alpha} \right)^{1/2} e^{-\omega^2/4\alpha}, \tag{6}$$

which, when substituted in (3), provides sufficient damping for reasonably large $\pm\omega$ to cause the spectrum of $u(\rho, \phi, t)$, i.e., $U(\rho, \phi, \omega)$, to be band-

limited for all practical purposes. This is desirable since the inverse Fourier transform generally can be performed only numerically. Thus, the analytical solution to the 90-degree wedge problem is obtained by substituting (6) into (3) and performing the operation in (4) numerically.

THE FINITE-DIFFERENCE FORMULATION

The homogeneous form of (1) can be approximated in rectangular coordinates by the explicit second-order difference scheme (Mitchell, 1969, p. 203):

$$\begin{aligned}
 u(m, n, l + 1) &= 2(1 - 2p^2)u(m, n, l) + p^2[u(m + 1, n, l) \\
 &+ u(m - 1, n, l) + u(m, n + 1, l) \\
 &+ u(m, n - 1, l)] \\
 &- u(m, n, l - 1) + O(h^2 + \Delta t^2),
 \end{aligned} \tag{7}$$

where $\Delta x = \Delta z = h$ is the grid size in the x and z directions, respectively; Δt is the time step; m, n, l are integers such that $x = m\Delta x, z = n\Delta z, t = l\Delta t$; $p = C_0\Delta t/h$; and $O(h^2)$ indicates the scheme approximates the corresponding partial differential equation to order h^2 . An alternate expression may be obtained by using the more accurate fourth-order representation for the Laplacian given by Abramowitz and Stegun (1964). The resulting difference scheme is

$$\begin{aligned}
 u(m, n, l + 1) &= (2 - 5p^2)u(m, n, l) \\
 &+ \frac{p^2}{12} \{ 16[u(m + 1, n, l) + u(m, n + 1, l) \\
 &+ u(m - 1, n, l) + u(m, n - 1, l)] \\
 &- [u(m + 2, n, l) + u(m, n + 2, l) \\
 &+ u(m - 2, n, l) + u(m, n - 2, l)] \} \\
 &- u(m, n, l - 1) + O(h^4 + \Delta t^2).
 \end{aligned} \tag{8}$$

A finite-difference scheme is said to be stable if the difference between the theoretical and numerical solutions of the difference equation remains bounded as l increases, Δt remaining fixed, for all m and n (Mitchell, 1969, p. 34). Equation (7) is known to be stable, provided that (Mitchell, 1969, p. 205)

$$p \leq 1/\sqrt{2}.$$

The same method may be used to show that (8) is stable if $p \leq \sqrt{3}/8$.

To obtain the appropriate source field $u_s(\rho, \phi, t)$ for use in the finite-difference method, the solution to (1) in an infinite free space is required. This is obtained as the inverse Fourier transform of the solution to equation (2) in an infinite free space (Morse and Feshbach, 1953, p. 891),

$$\begin{aligned}
 u_s(\rho, \phi, t) &= \frac{1}{2\pi} \int_{-\infty}^{+\infty} \{ -i\pi H_0^{(2)}(k|\rho - \rho_s|) \\
 &\cdot F(\omega) \} e^{+i\omega t} d\omega,
 \end{aligned} \tag{9}$$

where $F(\omega)$ is as defined by (6) and $|\rho - \rho_s|$ is the distance from the source to the observation point. The inverse Fourier transform necessary to obtain $u_s(\rho, \phi, t)$ is performed numerically. The source field power spectrum and the source field time response at a representative location are displayed in Figures 3a and 3b, respectively.

Problems in the finite-difference formulation arising from the area near the source location are handled by deleting the source contribution to the total velocity potential from a small square enclosing the source location. This approach was

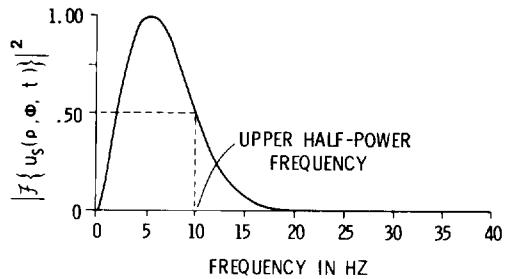


FIG. 3a. Normalized source field power spectrum at $\rho = 2000$ ft.

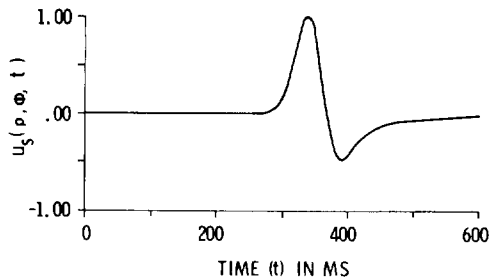


FIG. 3b. Normalized source field time response at $\rho = 2000$ ft.

used successfully by Alterman and Karal (1968). The overall size of the finite-difference model can be made sufficiently large to prevent distortion of the results by spurious reflections from the edges of the model.

RESULTS

Second-order scheme

A comparison of the finite-difference results for the second-order scheme of (7) with the analytical results obtained from the eigenfunction expansion method is shown in Figure 4 for three different receiver locations. Of particular interest is the observation that the diffraction (Figure 4c) is gen-

erated to good accuracy by finite-difference methods. An important parameter affecting the accuracy of finite-difference methods is grid coarseness. A measure of grid coarseness is the number of grid points per wavelength of the source; we shall use G_0 the number of grid points/half-power wavelength. The half-power wavelength is defined to be the wavelength corresponding to the frequency of the upper half-power point of the source field power spectrum (see Figure 3a). For the value of α used (1000), the half-power wavelength is approximately 800 ft. For $\Delta x = 72$ ft, chosen for Figure 4, $G_0 \approx 11$.

Figure 5 shows the comparison between the re-

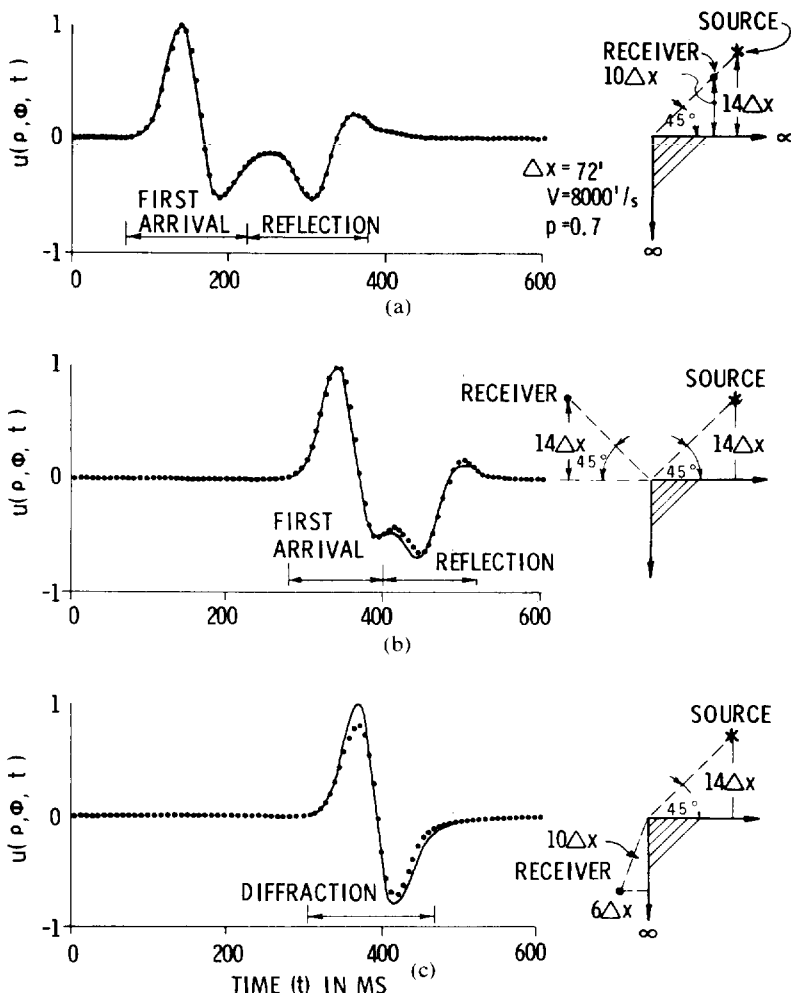


FIG. 4. Analytical solution (solid line) and fine grid ($G_0 \approx 11$) finite-difference solution (circles) for the second-order scheme.

examined by considering phase and group velocity as a function of frequency or, equivalently, as a function of G , the number of grid points/wavelength. The absence of dispersion would, of course, be characterized by phase velocities and group velocities that do not vary with frequency. Expressions for phase and group velocity based on plane wave propagation are developed in the appendix for the second-order finite-difference scheme represented by (7). Results from these equations are shown in Figure 6 for different values of θ the propagation angle with respect to the grid. Both the phase velocity C_P and the group velocity C_G are normalized to the zero-frequency phase velocity C_0 . It may be seen that dispersion is greatest when the wave propagates parallel to the grid ($\theta=0$). For this case the dispersion relation reduces to that for the corresponding one-dimensional, second-order, finite-difference scheme, i.e.,

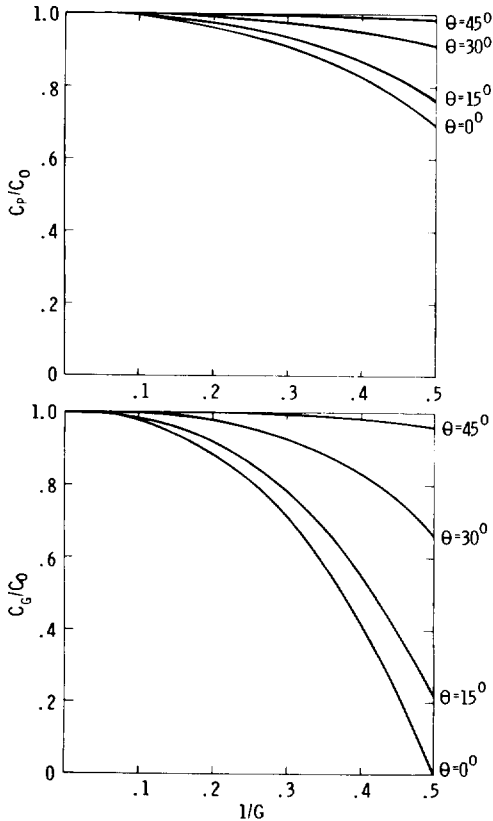


FIG. 6. Normalized phase and group velocity for different propagation angles with respect to the grid, for the second-order scheme ($p = .7$).

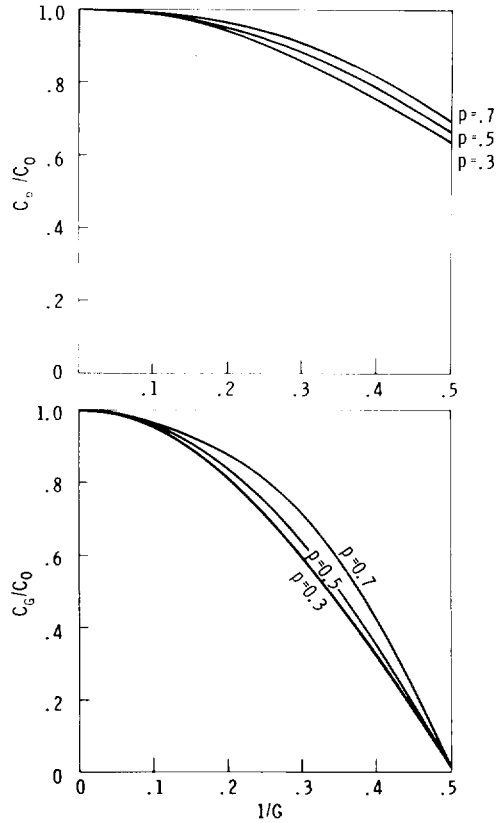


FIG. 7. Normalized phase and group velocity for different stability ratios for the second-order scheme.

$$\frac{C_P}{C_0} = \frac{G}{p\pi} \sin^{-1} \left(p \sin \frac{\pi}{G} \right), \quad (10)$$

$$\frac{C_G}{C_0} = \frac{\cos \pi/G}{(1 - p^2 \sin^2 \pi/G)^{1/2}}$$

Phase and group velocity curves for this case are shown in Figure 7 for various values of p . Figure 7 indicates that p should be made as large as possible to minimize dispersion. The maximum value is determined by the stability limit, $p=1/\sqrt{2}$. Using values of p near the stability limit is also desirable from the viewpoint of minimizing computational time.

Fourth-order scheme

Figure 8 shows a comparison of finite-difference calculations using the fourth-order scheme of (8) with the analytical results. It is striking that, al-

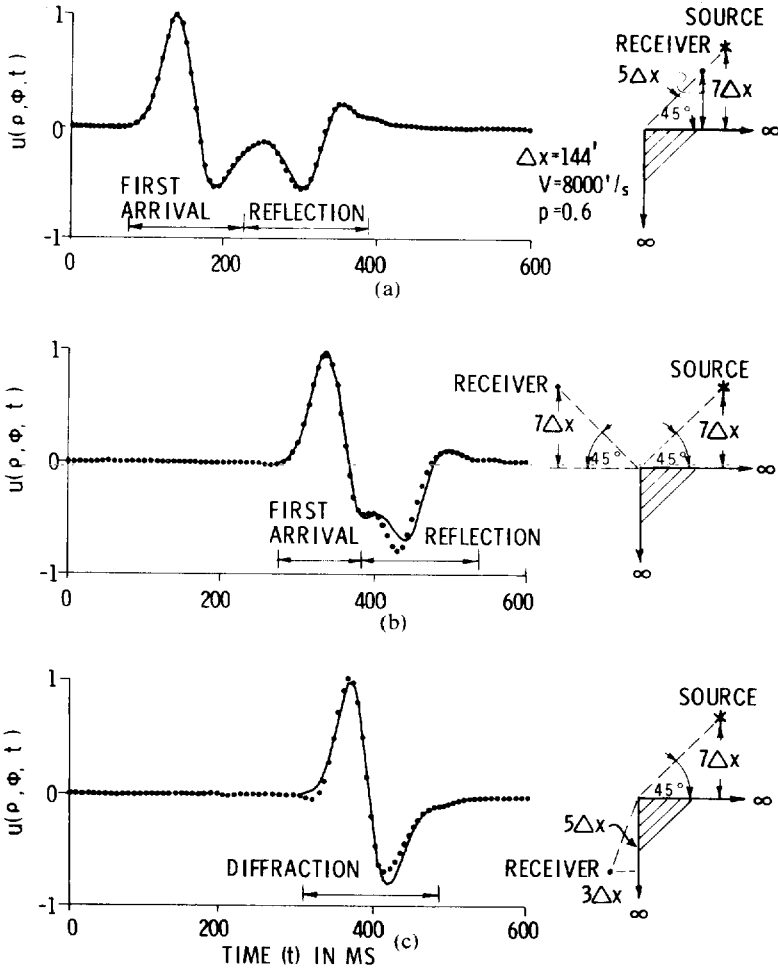


FIG. 8. Analytical solution (solid line) and coarse grid ($G_0 \approx 5.5$) finite-difference solution (circles) for the fourth-order scheme.

though the grid size corresponds to that of the second-order coarse grid (Figure 5), the results are comparable to those obtained from the second-order fine grid (Figure 4).

Expressions for phase and group velocity as a function of grid points per wavelength can be developed for the fourth-order, finite-difference scheme by the method used in the appendix. The results for the one-dimensional case are given by

$$\frac{C_P}{C_0} = \frac{G}{p\pi} \sin^{-1} \left\{ (1 + 1/3 \sin^2 \pi/G)^{1/2} p \sin \pi/G \right\}$$

$$\frac{C_G}{C_0} = \frac{(1 - \sin^2 \pi/G)^{1/2}}{[1 - (1 + 1/3 \sin^2 \pi/G) p^2 \sin^2 \pi/G]^{1/2}} \cdot \left\{ \frac{1 + 2/3 \sin^2 \pi/G}{(1 + 1/3 \sin^2 \pi/G)^{1/2}} \right\} \quad (11)$$

These expressions are plotted in Figure 9 for two different values of the parameter p . Velocity curves for the second-order expression with p near the stability limit are shown for comparison. It may be seen that less dispersion is predicted for the fourth-order scheme near its stability limit

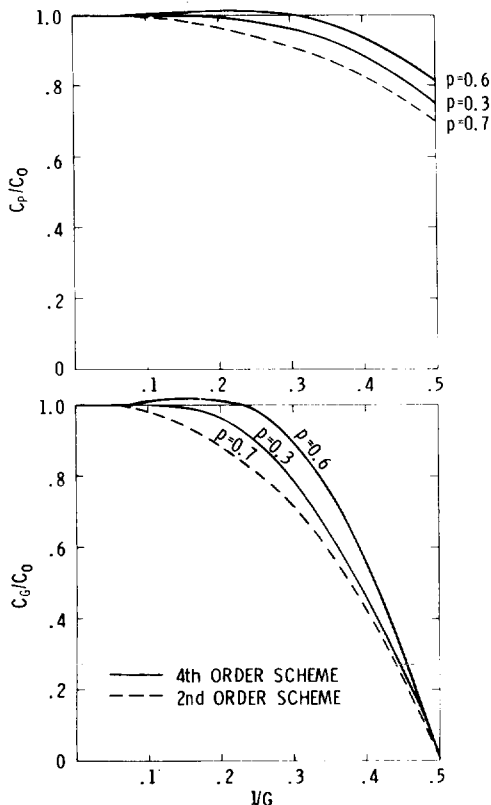


FIG. 9. Normalized phase and group velocity for different stability ratios for the fourth-order scheme ($\theta = 0$). Curves for the second-order scheme with $\rho = .7$ are shown for comparison.

($\rho \approx .6$) than for the second-order scheme at its stability limit ($\rho \approx .7$); this prediction is consistent with the results.

CONCLUSIONS

From the comparison described, it can be concluded that the finite-difference method yields accurate results for models containing sharp corners, provided that the grid is sufficiently fine. In the writers' opinion, ten or more grid points per wavelength at the frequency of the upper half-power point should be adequate when the usual second-order accuracy finite-difference scheme is em-

ployed, while the fourth-order scheme seems to produce accurate results at five grid points per wavelength at the frequency of the upper half-power point. The resulting savings in computer memory requirements and computational time are sufficient to justify the added complexity of the algorithm. If an insufficient number of grid points per wavelength is used, the grid dispersion effect leads to inaccurate results. It is important that one bear this in mind when using finite-difference methods for more complex structures where many closely spaced events are present, since grid dispersion can distort the results to a point where serious errors may be made in interpretation of the events.

ACKNOWLEDGMENTS

The grid dispersion analysis in this paper was motivated by unpublished work of D. J. Andrews. Helpful comments and suggestions by S. Treitel, R. W. Ward, and W. G. Clement are appreciated. Finally, thanks are due Amoco Production Co. for permission to publish this work.

REFERENCES

- Abramowitz, M., and Stegun, I. A., 1965, Handbook of mathematical functions: New York, Dover Publishing Co., p. 885.
- Alterman, Z., and Karal, F. C., Jr., 1968, Propagation of elastic waves in layered media by finite-difference methods: Bull. Seism. Soc. Am., v. 58, p. 367-398.
- Boore, D. M., 1970, Finite-difference solutions to the equations of elastic wave propagation, with application to Love waves over dipping interfaces: Ph.D. thesis, M.I.T.
- 1972, Finite-difference methods for seismic wave propagation in heterogeneous materials, in Methods in computational physics: B. Alder, S. Fernbach, and M. Rotenberg, editors, v. 2, New York, Academic Press, p. 21-22.
- Bowman, J. J., Senior, T. B. A., and Uslenghi, P. L. E., editors, 1969, Electromagnetic and acoustic scattering by simple shapes: New York, John Wiley & Sons.
- Mitchell, A. R., 1969, Computational methods in partial differential equations: New York, John Wiley & Sons.
- Morse, P. M., and Feshbach, H., 1953, Methods of theoretical physics: New York, McGraw-Hill Book Co., Inc.
- Oberhettinger, F., 1954, Diffraction of waves by a wedge: Commun. Pure Appl. Math., v. 7, p. 551-563.
- Ottaviani, Mario, 1971, Elastic wave propagation in two evenly welded quarter-spaces: Bull. Seism. Soc. Am., v. 61, p. 1119-1152.

APPENDIX

Expressions for phase and group velocity for the second-order finite-difference scheme will be developed in this appendix.

Consider harmonic plane wave propagation of the form

$$u = u_0 e^{i(\omega t - kx \cos \theta - kz \sin \theta)}, \quad (\text{A1})$$

where θ is the angle between the direction of propagation and the x -axis. If (A1) is substituted into (7) one obtains

$$\sin^2 \frac{\omega \Delta t}{2} = p^2 \left[\sin^2 \left(\frac{kh \cos \theta}{2} \right) + \sin^2 \left(\frac{kh \sin \theta}{2} \right) \right]. \quad (\text{A2})$$

Since $kh/2 = \pi/G$, (A2) can be written as

$$\frac{C_P}{C_0} \equiv \frac{\omega}{kC_0} = \frac{G}{p\pi} \sin^{-1} \left\{ p \left[\sin^2 \left(\frac{\pi \cos \theta}{G} \right) + \sin^2 \left(\frac{\pi \sin \theta}{G} \right) \right]^{1/2} \right\}. \quad (\text{A3})$$

For the limiting case of propagation parallel to the grid ($\theta=0$), (A3) reduces to the one-dimensional result

$$\frac{C_P}{C_0} = \frac{G}{p\pi} \sin^{-1} \left[p \sin \frac{\pi}{G} \right]. \quad (\text{A5})$$

The corresponding expression for group velocity is obtained by differentiation of (A2) with respect to k and is given by

$$\frac{C_G}{C_0} = \frac{\left[\sin \left(\frac{\pi}{G} \cos \theta \right) \cos \left(\frac{\pi}{G} \cos \theta \right) \cos \theta + \sin \left(\frac{\pi}{G} \sin \theta \right) \cos \left(\frac{\pi}{G} \sin \theta \right) \sin \theta \right]}{\left[1 - p^2 \sin^2 \left(\frac{\pi}{G} \cos \theta \right) - p^2 \sin^2 \left(\frac{\pi}{G} \sin \theta \right) \right]^{1/2} \left[\sin^2 \left(\frac{\pi}{G} \cos \theta \right) + \sin^2 \left(\frac{\pi}{G} \sin \theta \right) \right]^{1/2}}. \quad (\text{A6})$$

For the limiting case of propagation parallel to the grid, (A6) also reduces to the one-dimensional result

$$\frac{C_G}{C_0} = \frac{\cos \pi/G}{(1 - p^2 \sin^2 \pi/G)^{1/2}}. \quad (\text{A7})$$